

## EXPERIMENTAL AND NUMERICAL INVESTIGATION ON FLOW ANGLE CHARACTERISTICS OF AN AUTOMOTIVE MIXED FLOW TURBOCHARGER TURBINE

M. H. Padzillah<sup>a\*</sup>, S. Rajoo<sup>a</sup>, R. F. Martinez-Botas<sup>b</sup>

<sup>a</sup>UTM Centre for Low Carbon Transport in Cooperation with Imperial College London, Faculty of Mechanical Engineering, Universiti Teknologi Malaysia, Johor Bahru, Malaysia

<sup>b</sup>Department of Mechanical Engineering, Imperial College London, London SW7 2AZ, United Kingdom

### Article history

Received

20 July 2015

Received in revised form

23 September 2015

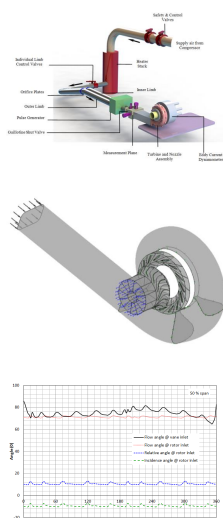
Accepted

22 October 2015

\*Corresponding author

mhasbullah@utm.my

### Graphical abstract



### Abstract

To date, turbocharger remains as a key enabler towards highly efficient Internal Combustion Engine. Although the first turbocharger was patented more than 30 years ago, the design is still being improved, thus signifying its importance in modern vehicles. One of the key features that contribute to the challenges in designing highly efficient turbine is the complex nature of the flow field within the turbine stage itself. Experimental method could be used to extract parameters such as pressure and temperature traces but still unable to provide a full description of the flow field. Therefore, the use of Computational Fluid Dynamics (CFD) in resolving this issue is necessary. Out of many feature of fluid flow in turbomachinery, the flow angle at rotor inlet plays significant role in determining turbine efficiency. However, due to geometrical complexity, even at optimum averaged incidence flow angle, there still exist variations that could impair the turbine ability to produce work. This research attempts to provide insight on the complexity of flow angle distribution within the turbocharger turbine stage. To achieve this aim, a numerical model of a full stage turbocharger turbine operating at 30000rpm under its optimum condition was developed. Results indicated that even though use of guide vanes has reduced flow angle fluctuations at mid-span of the rotor inlet from  $\pm 10^\circ$  to only  $\pm 1^\circ$ , significant variations still exist for velocity components in spanwise direction. This in turns effected the distribution of incidence flow angle at the rotor leading edge. In the current research, variation of incidence flow angle in spanwise direction is recorded to be as high as  $60^\circ$ .

**Keywords:** Mixed-flow turbine, computational fluid dynamics, pulsating flow

© 2015 Penerbit UTM Press. All rights reserved

## 1.0 INTRODUCTION

One of the early attempts to perform 3-D computational study on the turbocharger turbine was done by Lymberopoulos *et al.* [1] in 1988. In this work a simplified quasi-three-dimensional solution of the Euler equation was used. The radial and tangential components of velocity were fully solved, but the axial component was only treated to simulate the mixing of two streams. Lymberopoulos *et al.* validated the model with experimental results with good agreement. Although the model was not fully resolved in axial

direction, they concluded that significant variations in flow properties exist around the exit circumference of the volute.

The use of CFD is not limited only to understanding the flow field. Many studies used this tool to assist development of new turbine concepts. Barr and Spence [2] used CFD approach to develop a back swept turbine blade to improve turbine efficiency at low velocity ratios. They managed to obtain 2% efficiency improvement when compared to the original design. They also concluded that the back swept radial turbine performed less efficiently at high

velocity ratios. Barr *et al.* [3] later extended their work to include experimental validations. Despite that, the experimental data obtained could only cover half the operating points, and data at the lowest velocity ratios that were predicted to have the most significant improvements could not be captured.

Perhaps the more related literature to the current work is the work by Tamaki *et al.* [4]. They indicated that the existence of tip clearance especially at small vane opening, results in extensive wake flow and leakage vortex. This feature further distorts the total pressure distribution and flow angle which in turn caused mixing loss downstream of the nozzle vanes and the rotor, thus affecting its overall performance. Padzillah *et al.* [5] indicated that failure to precisely model the actual geometry could result in under prediction of static pressure distribution on the blade surfaces, thus the overall turbine performance cannot be accurately calculated. This results in erroneous prediction of flow pattern within the numerical domain hence the complex nature of the flow will not be accurately predicted.

This work aims to provide insight on the distortions of the flow velocity and its angle due to the complex nature of the turbocharger turbine stage geometry.

## 2.0 METHODOLOGY

### 2.1 Experimental Setup

Figure 1 shows the schematic of the turbocharger test facility used in this study. The facility is located at Imperial College London for cold-flow testing and could be used for steady and pulsating flow testing. For the current research, only steady flow cases were tested. The compressed air for the test rig is supplied by three screw-type compressors with capacity up to 1 kg/s at maximum absolute pressure of 5 bars. The air is heated by a heater-stack to temperatures between 330K to 345K to prevent condensation during gas expansion in the turbine. The flow is then channelled into two 81.40mm limbs, namely outer and inner limb due to its relative position. This enables testing not only for single entry turbine but also for double or twin entry turbine. The mass flow rate in both limbs is measured using orifice plates. Downstream to the orifice plates is a pulse generator originally designed by Dale and Watson [6] in 1986. The pulse generator enables actual pressure pulse in the exhaust manifold to be replicated in the facility with the frequency up to 80Hz. For the current research, the pulse generator is defaulted to 'fully open' position to allow maximum steady-state flow area. Downstream of the pulse generator is the 'measurement plane' where all the parameters for the turbine inlet were acquired including total and static pressure as well as temperature.

The turbine is attached to a 60kW eddy current dynamometer where it is placed on a gimbal bearing. Readers are referred to Szymko [7] for details of the eddy current dynamometer design. The reaction force on the dynamometer assembly is measured by a 20kg

load cell from where the torque is then calculated. The dynamometer also places a high flow rate water cooling system to disperse excessive heat absorbed by the magnetic plate. An optical sensor for instantaneous speed measurement is also installed within the dynamometer assembly.

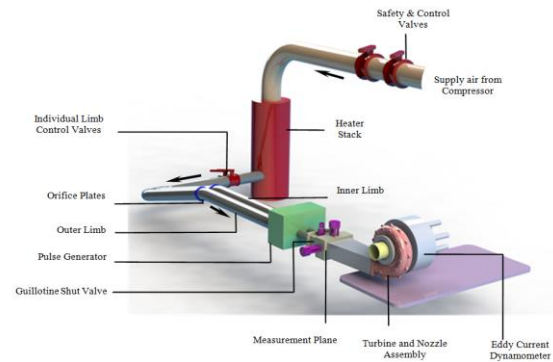


Figure 1 Imperial College 'cold flow' turbocharger test facility

### 2.2 Numerical Setup

The simulation works conducted in this research were executed using commercial software Ansys CFX 14.1. The 3-Dimensional turbocharger turbine geometry consists of 5 main components which are the inlet duct, a modified Holset H3B turbine volute [8], 15 NACA 0015 profiled vanes and a mixed flow turbine with 40mm chord length. The inlet duct and the volute were constructed using Solidworks and meshed using Ansys ICEM CFD. For the nozzle stage, 15 lean vanes were constructed by importing 3 profile lines into TurboGrid software where structured hexahedral meshing was automatically generated. Similar method was used to mesh the mixed flow turbine except 8 profile lines were needed due to its more complex geometry. The profile lines of the turbine blade were created using Bezier polynomial where its control points are shown in Figure 2. The turbine used was an in-house turbine designated Rotor A created by Abidat [9] in 1991 for applications in high loading operations. Figure 2(a) shows the resultant polynomial lines that forms the hub (blue line) and the shroud (red line) of the rotor wheel. The dotted line in Figure 2(a) indicated the imaginary position of the leading and trailing edge of the rotor. It can be seen that the overall chord length is 40 mm. Figure 2(b) shows the curvature of the leading edge and the camber line of the blade.

Subsequently, all meshed components were assembled in Ansys CFX-Pre as shown in Figure 3. The interfaces between each component are specified during this stage. The interfaces between inlet duct and volute, and also between volute to vane are specified as general connection. Frozen rotor interface is specified between vane and rotor domains. For steady state simulations, the use of frozen rotor interface is well justified as it will not impair accuracy of calculated model [10].

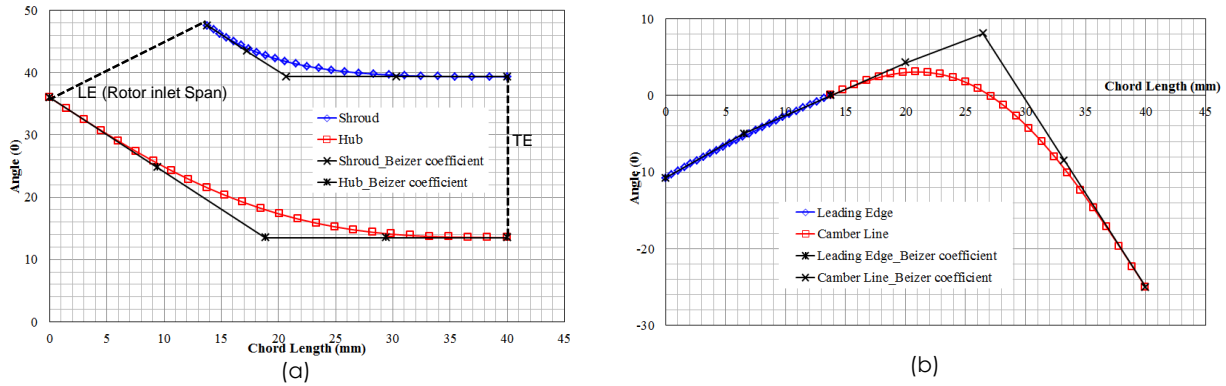


Figure 2 Development of turbine geometry using Bezier Polynomial

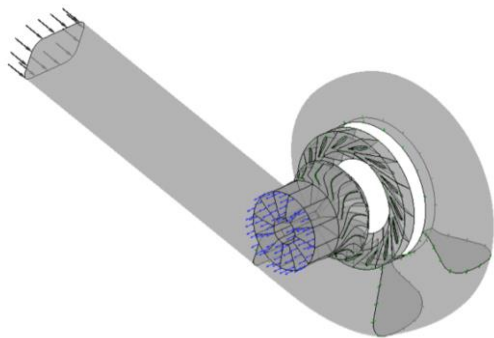


Figure 3 Assembly of domain in CFX-Pre

At the domain inlet (inlet duct), total pressure and total temperature were specified according to the turbine operating conditions. For the current case, the total pressure was set to be 304 kPa to produce a turbine pressure ratio of 1.3. Total temperature was set to be 333 K, a temperature similar to testing conditions. The direction of inlet flow was defined so that the only velocity component that exists is normal to the inlet plane. The outlet boundary condition requires the static pressure value. For this purpose, a constant atmospheric pressure was applied at the domain outlet. No-slip boundary condition was specified at all walls including vanes and rotor blades. The rotor speed was set to 30,000 rpm which is equivalent to 50% of the design speed. This particular speed was selected due to the availability of extensive experimental data which is valuable for model validation.

### 3.0 RESULTS AND DISCUSSION

#### 3.1 Validation Exercises

Before the analysis, the computed models were verified with experimental results. This procedure was done by computing the turbine performance parameters which are the turbine mass flow

parameters (also known as swallowing capacity), pressure ratio, efficiency and velocity ratio from CFD results and comparing them with available experimental data.

Figure 4(a) shows the plot of mass flow parameter against pressure ratio for the turbine rotating at 30,000 rpm. Both CFD and experimental data are plotted on similar axis to enable direct comparison. From the figure, it can be seen that the model used in this research are able to capture the trend and magnitude of the turbine mass flow parameter (also known as swallowing capacity) well for the entire operating range. The RMS of the deviation from experimental data is approximately 2%.

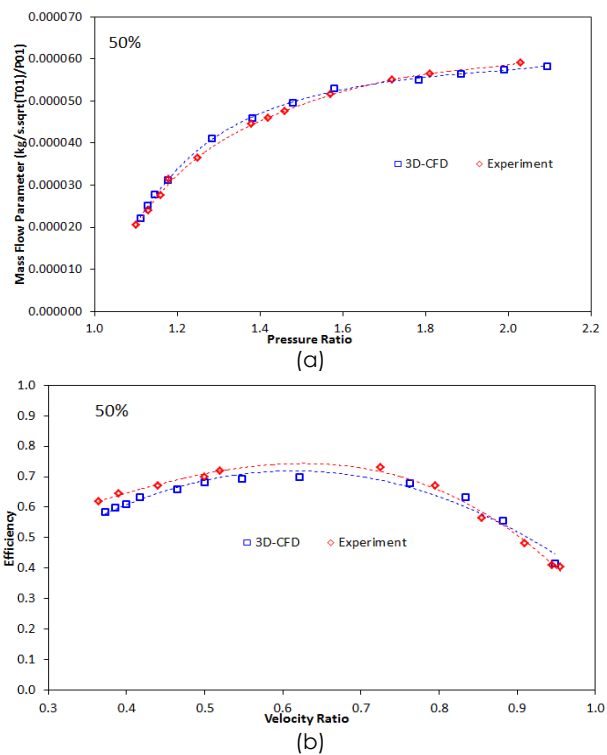


Figure 4 Comparison between CFD and Experimental data of (a) Mass Flow Parameter vs Pressure Ratio and (b) Efficiency vs Velocity Ratio

The validation procedure involving turbine efficiency has been proven to be more difficult since efficiency is a derived parameter. Therefore, it depends on accuracy of several calculated parameter such as mass flow rate, torque, temperature and pressure. In addition, the use of fixed values such as the turbine speed and specific heat ratios could also lead to over or under predictions of the turbine efficiency. Figure 4(b) shows the comparison between experimental data and CFD predictions of the turbine efficiency against velocity ratio. It can be seen that CFD tend to under predict the efficiency values for velocity ratios less than 0.85. The maximum deviation was recorded to be 5 efficiency points at the velocity ratio of 0.36. The RMS deviation recorded for this plot is 2 efficiency points. The small RMS deviations for both plots indicated that the developed model had achieved sufficient accuracy and as such could be used for further analysis.

### 3.2 Flow Angle Distributions

Figure 5 shows the plot of flow angle distribution against the circumferential location of the volute. The location where the flow angle at the volute exit was measured is detailed in Figure 6. From Figure 5, it can be clearly seen that the flow angle does not maintain a constant value but it fluctuates due to the proximity of the vanes. Maximum fluctuation is recorded close to the tongue region with the magnitude of  $\pm 10^\circ$ .

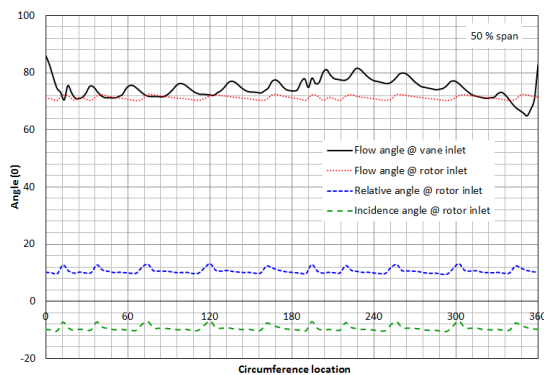


Figure 5 Flow angle at vane inlet and rotor inlet

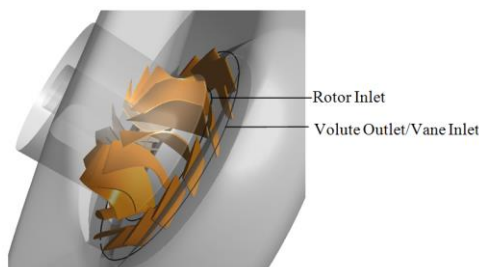


Figure 6 Location of data measurement at mid-span

As the flow passes through the vane, the flow angle variations across the circumferential location reduced significantly as compared to its variation at the volute

exit/vane inlet. At the exit of the vanes, only small localized fluctuations were detected due to proximity to the turbine wheel inlet. There was no evidence of wake flow from the vanes trailing edge that could be observed where the flow angle was measured. The magnitude of the mean flow angle was  $71^\circ$  with only  $\pm 1^\circ$  fluctuations. This observation shows that the current arrangement of vanes is sufficient to guide the flow and to minimize the substantial flow angle variations that occur at the volute exit. This ensures that the flow enters the rotor at a constant incidence angle which is very beneficial, provided that the incidence angle falls into its optimum range.

At the rotor inlet, the relative and incidence angles were also plotted in the same axis in Figure 5. In the current operating condition, the averaged incidence angle reads  $-10^\circ$  which is close to the optimum limit between  $-20^\circ$  to  $-30^\circ$  [11], hence the maximum efficiency for the particular operating speed.

Even though the vanes are capable of improving the flow angle distributions at the volute exit circumferentially, the complexity of the turbocharger turbine geometry prevents similar distributions of the flow angle in spanwise direction. Figure 7 shows the plot of velocity components along the span of the rotor inlet (see Figure 2(a)) at  $180^\circ$  circumferential location. From Figure 7, it can be seen that in general the flow turned into its primary direction which is the streamwise direction. This was indicated by the relatively high magnitude of the streamwise velocity as compared to the other velocity components. Along the span, it can also be seen that this velocity components varied by as much as 65 m/s where the maximum velocity that was recorded close to the shroud wall has the magnitude of 100 m/s. However, the magnitude of the streamwise velocity drops to 45 m/s at 0.85 spanwise location. This feature is labelled X in Figure 7. The sudden change in the velocity component over a relatively short distance was due to the blade tip clearance close to the shroud. The streamwise velocity then remains relatively constant at 50 m/s until 0.3 spanwise location. Closer to the hub, the velocity increases and peaks at 75 m/s before it drops again to 60 m/s at the hub proximity.

As for the spanwise velocity, a consistently negative value was recorded as shown in Figure 7. This feature indicated that there are fluid movements from hub to the shroud of the rotor inlet, and therefore impeding the primary flow which is in the streamwise direction. This condition was worst at about 0.05 spanwise location, close to the hub where the flow was moving from the hub to the shroud at 36 m/s. This behaviour occurs due to the geometry of the trailing edge of the vanes that has different radial distance from the centre of rotation in order to match the geometry of the mixed flow turbine. Therefore, as the flow enters the turbine wheel, it turns from radial to axial direction earlier at the shroud than the hub. This in turns induces flow movement from hub to shroud at the leading edge of the rotor.

For the tangential velocity component, there is a strong change from a negative value at the shroud to



a positive value at about 0.85 span location (labelled X in Figure 7). This behaviour is associated with the reduction of Coriolis acceleration that is acting on the fluid as it enters the rotating domain. Japikse and Baines [11] indicated that the decreasing radius of the rotor causes uneven cross-passage forces between the shroud and hub at the rotor. At negative incidence angles such as the current operating condition, this behaviour resulted in a secondary flow in the blade passage in the form of a circulation in the opposite direction to the passage rotation. For the current operating condition, the maximum difference of tangential velocity component as seen in Figure 7 is 85 m/s, which is a significant difference. Furthermore, close to the hub (less than 0.1 span location), the tangential velocity reduces to a relatively negligible values.

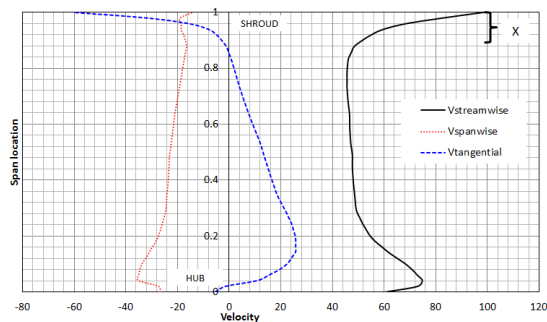


**Figure 7** Velocity components distributions across the span length of the rotor leading edge

As the velocity components vary across the span of the rotor inlet, so does the flow angles. Figure 8 shows the plot of the absolute, relative and incidence flow angles across the spanwise location at  $180^\circ$  inlet of the rotor. It can be seen from Figure 8 that for the absolute flow angle, the value of  $71^\circ$  holds for most of the span length (from 0.22 to 0.90). However, close to the shroud wall, the flow angle reduces to  $40^\circ$ . Figure 8 also clearly shows that the incidence angle changes substantially from hub to shroud. Close to the shroud, it has a very negative value of about  $-52^\circ$ , which is a very large deviation from optimum incidence angle. Towards the hub, the incidence angle becomes less

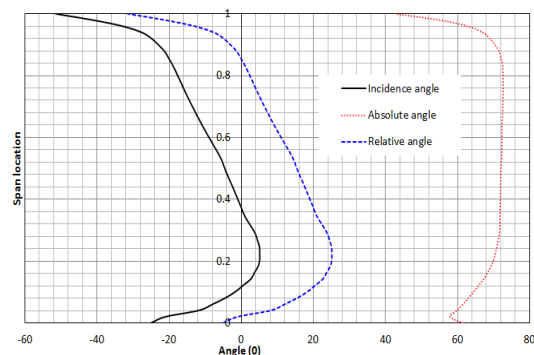


**Figure 8** Flow angle components distributions across the span of rotor leading edge

negative and turns to a positive value at about 0.4 span location. This flow angle levels-off at 0.2 span with the value of  $5^\circ$  and then reduces back to  $-25^\circ$  at hub.

## 4.0 CONCLUSION

The numerical model for a full stage turbocharger turbine was successfully modelled and validated. The maximum RMS recorded for comparison of CFD and experimental data for both mass flow parameter and efficiency is 2%. The results indicated that in steady state condition, the use of guide vanes has positive effect in minimizing flow angle fluctuations at the rotor leading edge. However, due to geometrical complexity of the turbine, significant variations in flow angle distribution can be seen in streamwise, spanwise and also tangential direction. For the entire span length of the rotor inlet, the streamwise velocity recorded the highest velocity change which is 50 m/s. As the velocity components change significantly, the incidence flow angle was also affected. This study had shown that across the span of the rotor leading edge, the incidence flow angle changes abruptly in the range of  $60^\circ$  despite its average value of  $-9.8^\circ$ . This clearly shows that only part of the turbine span is operating under optimum condition. It also indicated that in the analysis involving flow within a mixed-flow turbine, one needs to be vigilant on averaging the flow parameter at the turbine leading edge. For cases that involve substantial spanwise variations, an average value does not fully representative of the actual conditions.

## Acknowledgement

The corresponding authors would like to acknowledge Universiti Teknologi Malaysia (VOT number: Q.J130000.272401K70) for the financial support to conduct this research.

## References

- [1] Lymberopoulos, N., Baines, N.C. and Watson, N. 1988. Flow in Single and Twin Entry Radial Turbine Volute. *ASME Gas Turbine Aeroengine Congr.* 88-GT-59.
- [2] Barr, L. and Spence, S.W.T. 2008. Improved Performance of a Radial Turbine Through the Implementation of Back Swept Blading. *Proc ASME Turbo Expo No. GT2008-50064.*
- [3] Barr, L., Spence, S., Thornhill, D. and Eynon, P. 2009. A Numerical and Experimental Performance Comparison of an 86 MM Radial and Back Swept Turbine. *Proc ASME Turbo Expo No. GT2009-59366.*
- [4] Tamaki, H., Goto, S., Unno, M. and Iwakami, A. 2008. The Effect of Clearance Flow of Variable Area Nozzles on Radial Turbine Performance. *Proc ASME Turbo Expo No. GT2008-50461.*
- [5] Padzillah, M.H., Rajoo, S. and Martinez-Botas, R.F. 2014. Influence of Speed and Frequency Towards the Automotive Turbocharger Turbine Performance under Pulsating Flow Conditions. *Energy Convers. Manag.* 80: 416–428.
- [6] Dale, A. and Watson, N. 1986. Vaneless Radial Turbocharger Turbine Performance. *Proc. IMechE Int. Conf. Turbocharging Turbochargers (Mechanical Eng. Publ. London).* 65–76.

- [7] Szymko, S. 2006. *The Development of an Eddy Current Dynamometer for Evaluation of Steady and Pulsating Turbocharger Turbine Performance*. PhD Thesis. Imperial College of Science, Technology and Medicine, University of London.
- [8] Rajoo, S. 2007. *Steady and Pulsating Performance of a Variable Geometry Mixed Flow Turbocharger Turbine*. PhD Thesis. Imperial College of Science, Technology and Medicine, University of London.
- [9] Abidat, M. 1991. *Design and Testing of a Highly Loaded Mixed Flow Turbine*. PhD Thesis. Imperial College of Science, Technology and Medicine, University of London.
- [10] Padzillah, M. H., Rajoo, S. and Martinez-Botas, R. F. 2012. Numerical Assessment of Unsteady Flow Effects on a Nozzled Turbocharger Turbine. *Proc ASME Turbo Expo No. GT2012-69062*.
- [11] Japikse, D. and Baines, N.C. 1994. *Introduction to Turbomachinery*. Michigan: Concepts ETI.
- [12] Rajoo, S. and Martinez-Botas, R. 2006. Experimental Study on the Performance of a Variable Geometry Mixed Flow Turbine for Automotive Turbocharger. *Proc. IMechE Int. Conf. Turbochargers Turbocharging (Mechanical Eng. Publ. London)*. 183–192.